# Optical and structural properties of LaF₃ thin films

Martin Bischoff,[1,2,*] Dieter Gäbler,[2] Norbert Kaiser,[2] Andrey Chuvilin,[3] Ute Kaiser,[3]
and Andreas Tünnermann[1,2]

[1]Friedrich-Schiller-University, Institute of Applied Physics, Max-Wien-Platz 1, 07743 Jena, Germany
[2]Fraunhofer Institute for Applied Optics and Precision Engineering, Albert-Einstein-Strasse 7, 07745 Jena, Germany
[3]University of Ulm, Electron Microscopy Group of Materials Science, Albert-Einstein-Allee 11, 89081 Ulm, Germany

*Corresponding author: martin.bischoff@iof.fraunhofer.de

LaF₃ thin films of different thicknesses were deposited on $CaF_2$ (111) and silicon substrates at a relatively low substrate temperature of 150 °C. Optical (transmittance, reflectance, refractive index, and extinction coefficient) and mechanical (morphology and crystalline structure) properties have been investigated and are discussed. It is shown that LaF₃ thin films deposited on $CaF_2$ (111) substrates are monocrystalline and have a bulklike dense structure. Furthermore, it is presented that low-loss LaF₃ thin films can be deposited not only by boat evaporation but also by electron beam evaporation.  © 2008 Optical Society of America

*OCIS codes:*   310.0310, 310.6870.

## 1. Introduction

Lanthanum fluoride (LaF₃) is a highly refractive layer material commonly used for deep UV and vacuum UV applications because of its high transparency in these wavelength ranges. The ArF lithography technology requires a minimization of optical losses due to scattering and absorption; consequently ample research has been conducted to optimize the coating process of LaF₃ and other fluorides. Thus, various deposition methods were examined [1–4], and the LaF₃ thin films fabricated by boat evaporation were found to show the lowest absorption in the vacuum UV spectral range [5]. Depending on the substrate temperature, LaF₃ is inhomogeneous, has a rough surface, and a polycrystalline structure.

However, the properties of LaF₃ are affected not only by the deposition methods, their parameters (temperature and deposition rate), and the vacuum conditions [6], but also by the substrate material and surface quality. According to [7], LaF₃ grows heteroepitaxially on $CaF_2$ (111) substrates, with the [00$l$] planes of LaF₃ being parallel to [111] of $CaF_2$. Furthermore, the LaF₃ films have a bulklike dense structure. In this study, the mechanical, structural, and optical properties of LaF₃ thin films of different thicknesses, deposited by boat and electron beam evaporation on $CaF_2$ of varied polish quality [with (111) and random orientation] and on silicon substrates, were examined.

## 2. Experiment

LaF₃ films with a thickness of 15, 30, 50, and 150 nm were fabricated by Mo-boat evaporation, and for comparison, a 150 nm LaF₃ film was deposited by electron beam evaporation. The background pressure was less than $10^{-6}$ mbar ($10^{-6}$ hPa), the substrate temperature 150 °C, and the deposition rate 0.2 nm/s. As the starting material, highly pure and high-quality low-oxide LaF₃ (Merck) was used. Single-crystal $CaF_2$ substrates [diameter 1 in. (1 in. = 2.54 cm) and thickness 2 mm] with an rms roughness (by atomic force microscopy, AFM) of less than 0.2 nm (superpolish $CaF_2\_s$) and 0.8 nm (normal polish $CaF_2\_n$) were cleaned manually with alcohol and acetone, because the roughness would increase extremely during ultrasonic cleaning. One kind of $CaF_2$ substrate surface had (111) planes with an accuracy of ±2°; the other had random orientation. The silicon

| Sample | Deposition Technique | Substrate Kind | Film Thickness (nm) | Measurements |
|---|---|---|---|---|
| A1–A4 | Mo-boat evaporation | Superpolish $CaF_2\_s$ | 15 | AFM, XRD, GI-XRD |
| B1 | Mo-boat evaporation | Superpolish $CaF_2\_s$ (111) | 30 | TEM, AFM, GI-XRD |
| B2 | Mo-boat evaporation | Superpolish $CaF_2\_s$ (random) | 30 | AFM, GI-XRD |
| B3 | Mo-boat evaporation | Normal polish $CaF_2\_n$ (111) | 30 | TEM, AFM, GI-XRD |
| B4 | Mo-boat evaporation | Si | 30 | GI-XRD |
| C1–C4 | Mo-boat evaporation | Si | 50 | AFM, GI-XRD |
| D1 | Mo-boat evaporation | Superpolish $CaF_2\_s$ (111) | 150 | R, T, IR, TEM, AFM, GI-XRD |
| D2 | Mo-boat evaporation | Superpolish $CaF_2\_s$ (random) | 150 | R, T, IR, AFM, GI-XRD |
| D3 | Mo-boat evaporation | Normal polish $CaF_2\_n$ (111) | 150 | R, T, IR, TEM, AFM, GI-XRD |
| D4 | Mo-boat evaporation | Si | 150 | XRD, GI-XRD |
| E | Electron beam evaporation | Superpolish $CaF_2\_s$ (111) | 150 | R, T, IR, AFM, GI-XRD |

substrates had a thickness of 340 μm and a diameter of 3 in.

The crystalline structure of the substrates and the $LaF_3$ films were investigated by x-ray diffraction (XRD, Bruker D 5005), and the mass density and surface roughness by grazing-incidence x-ray diffraction (GI-XRD). For comparison, the roughness was also analyzed by AFM measurement. The morphology of the 30 and the 150 nm films was investigated by transmission electron microscopy (TEM). Transmission and reflection spectra of the 150 nm $LaF_3$ samples were measured with a Lambda 850 (Perkin Elmer) spectrometer in the range of 175–300 nm, whereas the measuring device was purged continuously with $N_2$ gas to avoid photoabsorption of oxygen, moisture, and organic contamination. IR spectra were measured with a Fourier transform IR spectrometer (Varian 3100).

A summary describing the samples and the performed and presented measurements is shown in Table 1.

## 3. Results and Discussion

The crystalline structure of 15 nm $LaF_3$ films deposited on different $CaF_2$ substrates (samples A1–A3) is shown in Fig. 1(a). As presented in [7], [00$l$] planes of $LaF_3$ deposited on $CaF_2$ (111) are parallel to [111] of $CaF_2$, irrespective of polish quality. $LaF_3$ deposited on $CaF_2$ with random orientation (sample A2) seems to be amorphous, but it is also possible that the [00$l$] planes of $LaF_3$ are parallel to [111] of $CaF_2$. However, with only the help of a monocrystal XRD, which tilts and rotates the probe, the random plane orientation of $LaF_3$ and $CaF_2$ could be observed and defined. However, $LaF_3$ films 30, 50, and 150 nm thick show the same characteristics as Fig. 1(a). By contrast, $LaF_3$ deposited on silicon grows polycrystallinely. The crystalline structure is clearly observable for sample A4 [Fig. 1(b)].

To understand the effect of the substrate on the microstructure and the morphology of the thin films, the 30 nm (samples B1 and B3) and the 150 nm (samples D1 and D3) $LaF_3$ films were analyzed by TEM measurements. Even though the normal and the su-

perpolished $CaF_2$ substrates have the same crystalline orientation, the morphology is different. As is shown in Fig. 2(a), the film of sample D3 grows columnarly with pores and has a high surface roughness and a nanocrystalline structure with varied orientation of the crystallites. Furthermore, the substrate is monocrystalline with partial subsurface damage. In contrast to that, the film of sample D1 grows primarily monocrystalline without pores. But as is presented in Fig. 2(b), the $LaF_3$ film has nodular defects, starting at a thickness of approximately 20 nm. Further results were given by the high-resolution TEM analysis of 30 nm $LaF_3$ layers (sam-
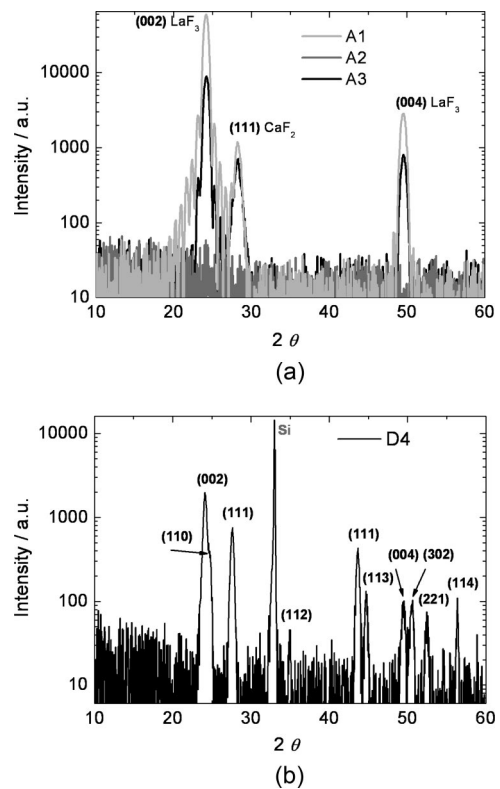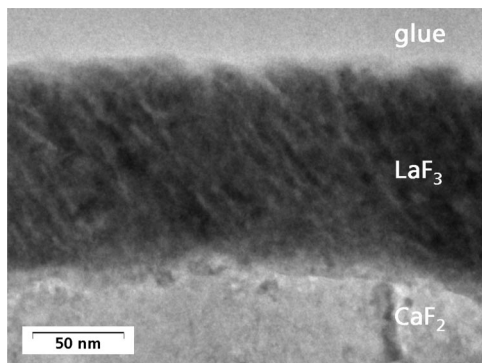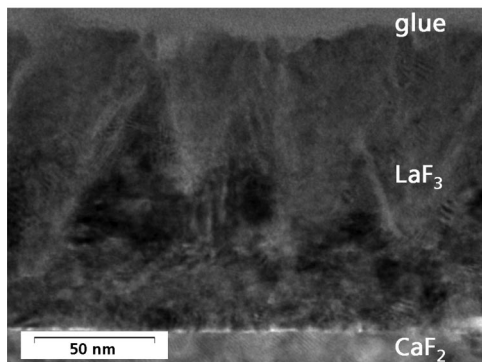




Fig. 1. XRD patterns from $LaF_3$ films: (a) 15 nm on different $CaF_2$ substrates; (b) 150 nm on Si substrate.

Fig. 2. TEM analysis (a) of sample D1 with nodular defects and (b) of sample D3 with columnar growth.





Fig. 3. High-resolution TEM analysis of (a) sample B1 and (b) sample B3.
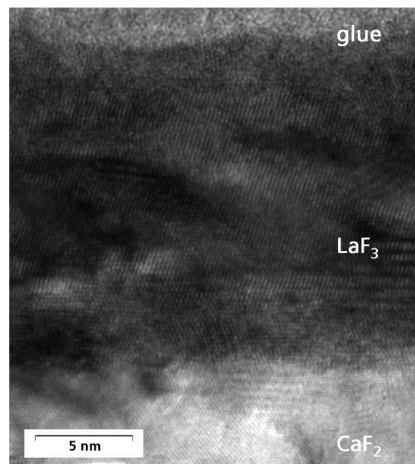
ples B1 and B3). But the effect of the substrate polish quality on the 30 nm films is less than expected. Both layers grow epitactically, are primarily monocrystalline, and have few incorrect crystal orientations, as is depicted in Fig. 3. These incorrect orientations caused by the slight mismatch of the crystalline structures of $LaF_3$ [00$l$] and $CaF_2$ (111) result in the columnar and nodular defects observed in the 150 nm $LaF_3$ films.

Figure 4 shows the development of surface roughness and surface morphology of $LaF_3$ thin films on $CaF_2$_$s$ analyzed by AFM measurements of $1 \times 1$ $\mu m^2$ areas. Because of the increasing size and number of columnar structures with increasing film thickness, rms roughness grows from 0.2 nm (substrate roughness) to 3.2 nm (sample D1). The highest roughness was measured at sample D3 with 5.2 nm.

The mass density and the roughness of $LaF_3$ films deposited on different substrates versus the film thickness are presented in Fig. 5. In comparison with the results from AFM analysis, rms roughness was also determined by GI-XRD measurements. Note that GI-XRD measurements of 150 nm thick $LaF_3$ films were difficult to analyze because of the limited penetration depth of x-rays in grazing-incidence configuration. Furthermore, layer inhomogeneity and subsurface damage were left out of consideration by the evaluation method.

However, it is obvious that $LaF_3$ films grow with a bulklike mass density on $CaF_2$ (111) substrates. But because of the relative low substrate temperature of 150 °C and the consequently lower surface mobility of $LaF_3$ molecules, the film becomes inhomogeneous with increasing thickness. The film of sample D3 shows the lowest mass density, whereas the films of samples D1 and D2 look similar to each other. The mass density of films on silicon substrates (samples A4–D4) decreases continuously, though with a smaller gradient.

The surface roughness of $LaF_3$ films on $CaF_2$ (111) substrates determined by GI-XRD measurements is clearly lower than the roughness of films on other substrates. But the comparison with rms roughness values determined by AFM is limited because of the subsurface damage of $LaF_3$ films, which is taken into account by GI-XRD, and the difference of the spatial frequencies of both methods. In comparison to these results for $LaF_3$ thin films prepared by boat evaporation, the 150 nm film deposited by electron beam evaporation (sample E) is outstanding. The results
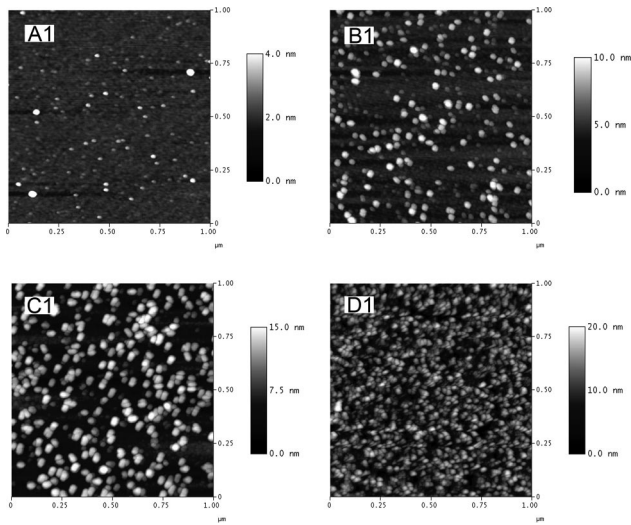
Fig. 4. Surface morphology of LaF$_3$ thin films of different thickness deposited on CaF$_2$_s (111) measured by AFM.
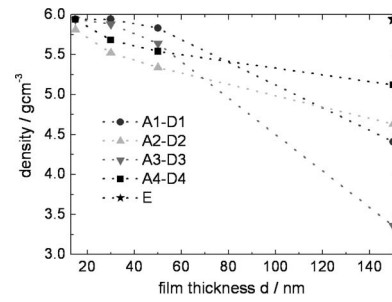
from GI-XRD show that the film has complete bulk density and has a very low surface roughness of only 0.5 nm.

The roughness of the films prepared by boat evaporation measured by the highly resolved AFM scans is correlated to film porosity, resulting in reduced density for 150 nm thick LaF$_3$ layers. However, in order to estimate the influence of roughness on scattering properties, a thoughtful roughness characterization with respect to the relevant spatial frequencies is necessary [8].
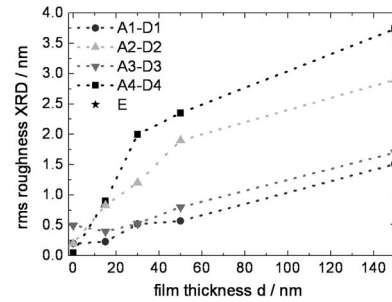
IR spectra of 150 nm LaF$_3$ films confirm the results of XRD and AFM. Thus, in comparison with sample D2, samples D1 and E have the lowest water content (Fig. 6) because of the bulklike dense film structure near the substrate, whereas sample D3 shows higher water content due to its higher film inhomogeneity. Because of the bulk density of the LaF$_3$ layer of sample E, the film has no water content at all.

For analysis of the reflection (R) and transmission (T) measurements (Fig. 7) and calculation of the optical constants in the UV region, a first-order bulk inhomogeneity (Schroeder model) was assumed. As a result, the refractive index of the films of samples D1 and D2 at a wavelength of 193 nm is 1.64 with an inhomogeneity factor $Q(z)$ of 9%. Furthermore, both layers have an extinction coefficient of less than $5 \times 10^{-4}$, which was confirmed by laser calorimetry measurements (Laser Zentrum Hannover). The film of sample D3 has a refractive index of 1.60 with a $Q(z)$ of more than 16% and an extinction coefficient of $2 \times 10^{-3}$. However, the best optical performance is given by sample E. The layer has a refractive index of 1.72, an extinction coefficient of less than $3 \times 10^{-4}$, and no inhomogeneity, as is presented by the reflectance spectra in Fig. 7(b) in comparison with the substrate reflection.
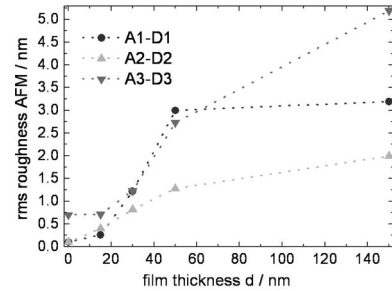
The difference between samples D1, D2, and E, referring to the absorption, is caused by the evaporation technique. As is presented in Fig. 7(a), the films

(a)



(b)



(c)

Fig. 5. (a) Mass density of LaF$_3$ films deposited on different substrates; corresponding surface roughness by (b) GI-XRD and (c) AFM.

prepared by Mo-boat evaporation have a characteristic absorption behavior that is mainly due to the boat material molybdenum. It was determined by examination that the Mo reacts with the layer mate-
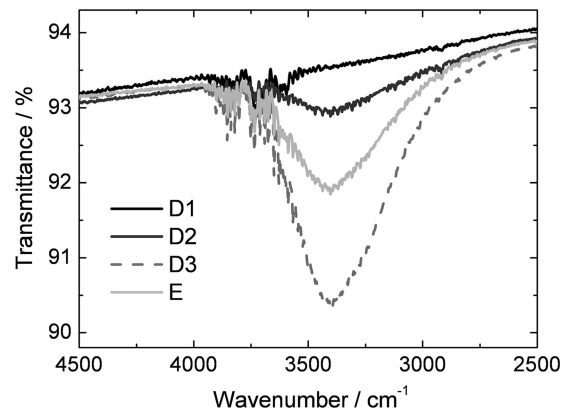


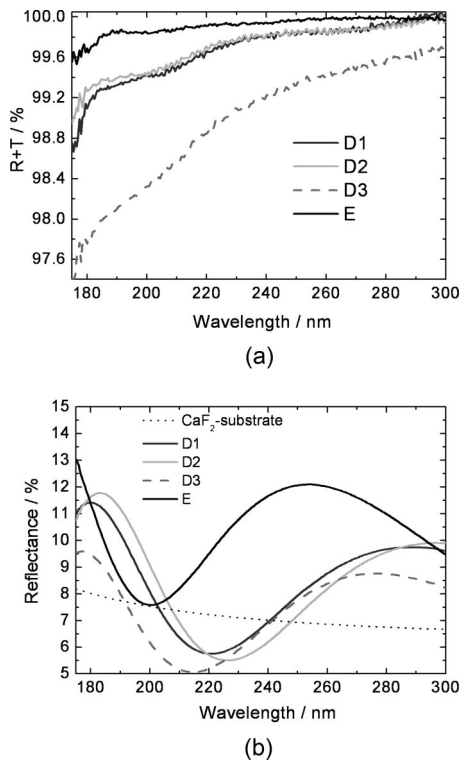Fig. 6. IR measurement of 150 nm LaF$_3$ layers.

Fig. 7. Spectral photometry (a) R + T and (b) R measurement of 150 nm LaF$_3$ layers.

rial inside the heated boat to yield MoF$_x$ (with $x = 3 \ldots 6$). This material is evaporated and integrated into the film structure and causes defects and the observed absorption at the wavelength of around 210 nm.

This assumption is supported by additional experiments: MoF$_x$ layers were deposited by heating an empty Mo-boat under the influence of fluorine gas with the flow of 30 sccm (sccm denotes cubic centimeters per minute at standard temperature and pressure). As a result, the F reacts with the heated boat material to yield MoF$_x$, which evaporates and forms a film of nearly pure MoF$_x$. The absorption of this film has its maximum at a wavelength of 210 nm. However, these experiments should not be discussed in detail at this point.

Consequently, the advantage of the electron beam technique is that no heated metal has direct contact with the evaporated layer material.

## 4. Conclusion

In this study, experiments with LaF$_3$ films deposited by boat and electron beam evaporation on different substrates at a substrate temperature of 150 °C have been analyzed and discussed. The investigation revealed bulklike dense films on CaF$_2$ (111) substrates up to a thickness of 50 nm, whereas 150 nm LaF$_3$ films prepared by boat evaporation were inhomogeneous, depending on the polish quality of the substrates. The film prepared by electron beam evaporation has complete bulk density, no inhomogeneity, no water content, a high refractive index and a very low extinction coefficient. It was shown that optical constants do not depend on the crystalline orientation of the CaF$_2$, but on the polish quality of the substrate. Thus, LaF$_3$ films deposited on superpolished CaF$_2$ substrates had the highest refractive index and also the lowest extinction coefficient.

## References

1. D. Ristau, S. Gunster, S. Bosch, A. Duparre, E. Masetti, J. Ferre-Borrull, G. Kiriakidis, F. Peiro, E. Quesnel, and A. Tikhonravov, "Ultraviolet optical and microstructural properties of MgF$_2$ and LaF$_3$ coatings deposited by ion-beam sputtering and boat and electron-beam evaporation," Appl. Opt. **41,** 3196–3204 (2002).
2. K. Iwahori, M. Furuta, Y. Taki, T. Yamamura, and A. Tanaka, "Optical properties of fluoride thin films deposited by RF magnetron sputtering," Appl. Opt. **45,** 4598–4602 (2006).
3. M.-C. Liu, C.-C. Lee, M. Kaneko, K. Nakahira, and Y. Takano, "Microstructure-related properties at 193 nm of MgF$_2$ and GdF$_3$ films deposited by a resistive-heating boat," Appl. Opt. **45,** 1368–1374 (2006).
4. C.-C. Jaing, M.-H. Shiao, C.-C. Lee, C.-J. Lu, M.-C. Liu, C.-H. Lee, and H.-C. Chen, "Effects of ion assist and substrate temperature on the optical properties and microstructure of MgF$_2$ films produced by e-beam evaporation," Proc. SPIE **5870,** 58700F (2005).
5. G. Atanassov, J. Turlo, J. K. Fu, and Y. S. Dai, "Mechanical, optical and structural properties of TiO$_2$ and MgF$_2$ thin films deposited by plasma ion assisted deposition," Thin Solid Films **342,** 83–92 (1999).
6. M.-C. Liu, C.-C. Lee, M. Kaneko, K. Nakahira, and Y. Takano, "Microstructure related properties of lanthanum fluoride films deposited by molybdenum boat evaporation at 193 nm," Thin Solid Films **492,** 45–51 (2005).
7. Y. Taki and K. Muramatsu, "Hetero-epitaxial growth and optical properties of LaF$_3$ on CaF$_2$," Thin Solid Films **420–421,** 30–37 (2002).
8. S. Schroeder, M. Kamprath, and A. Dupparé, "Characterization of thin films and bulk materials for DUV optical components," Proc. SPIE **6403,** 64031L (2007).